Superlattices and Microstructures 133 (2019) 106202

Contents lists available at ScienceDirect

Superlattices and Microstructures

journal homepage: www.elsevier.com/locate/superlattices

An investigation on structural, morphological, optical and third order nonlinear properties of facilely spray pyrolysis fabricated In: CdS thin films

Mohd Shkir [a,*], Mohd Anis [b], S.S. Shaikh [c], S. AlFaify [a,**]

[a] Advanced Functional Materials & Optoelectronics Laboratory (AFMOL), Department of Physics, Faculty of Science, King Khalid University, P.O Box-9004, Abha, 61413, Saudi Arabia
[b] Department of Physics and Electronics, Maulana Azad College of Arts, Science and Commerce, Aurangabad, 431001, Maharashtra, India
[c] Thin Film Physics Laboratory, Department of Physics, Electronics and Photonics, Rajarshi Shahu Mahavidyalaya, Latur, 413512 Maharashtra, India

ARTICLE INFO

Keywords:
CdS
Thin films
Optical properties
Dielectric and electrical properties
Z-scan
Third order nonlinear properties

ABSTRACT

Owing to the tremendous applications of cadmium sulphide (CdS), the fabrication of different content of In doped (0.0, 0.5, 1.0, 2.5 and 5.0 wt%) CdS thin films has been carried out facilely by spray pyrolysis technique. X-ray diffraction and FT-Raman studies confirm the single phase of CdS with hexagonal crystal system. The Scherrer rule was employed to determine the crystallite size and found to be reduced from 20 to 18 nm. The elemental composition and mapping studies shows that the prepared films contain In in CdS which is homogeneously distributed all over the film. The surface morphology was studied and noticed to be modified with increasing the content of In doping. The emission spectra were recorded at $\lambda_{exc} = 450$ nm and an intense green emission was observed at 529 ± 16 nm for pure and In:CdS films. The optical study reveal that the optical transparency is enhanced from 65% to 75% with In doping. The refractive index was noticed in range from 1 to 2.8. The direct optical energy gap was estimated in the range from 2.31 to 2.46 eV and shows reduction with In content. The open and closed aperture Z-scan measurement was carried out and nonlinear absorption, third order nonlinear susceptibility and refractive index values were determined and found in range from 3.12×10^{-3} to 5.37×10^{-3} cm/W, 4.67×10^{-1} to 7.01×10^{-1} esu and 2.14×10^{-7} to 5.99×10^{-7} cm^2/W, correspondingly.

1. Introduction

Indium as dopant is found to be an exceptional element specially in semiconductors as well as other materials to modify the physical properties for future device applications [1,2]. It is well-known that by adding the impurities to a semiconductor of wide energy band gap leads to modify the optoelectrical and nonlinear characteristics intensely [2–5]. Among several semiconductors' cadmium sulphide (CdS) is noticed to be an excellent candidate for various device applications such as: window layer material for solar/dye sensitized solar cell, photodetector, FET, lasers, etc. [6–13]. CdS possess two crystal structures as hexagonal wurtzite the most stable form and cubic zinc blende structures which are obtained from Greenockite and Hawleyite minerals.

* Corresponding author.
** Corresponding author. King Khalid University, Abha, Saudi Arabia.
E-mail addresses: shkirphysics@gmail.com (M. Shkir), saalfaify@kku.edu.sa (S. AlFaify).

https://doi.org/10.1016/j.spmi.2019.106202
Received 7 July 2019; Received in revised form 16 July 2019; Accepted 19 July 2019
Available online 24 July 2019

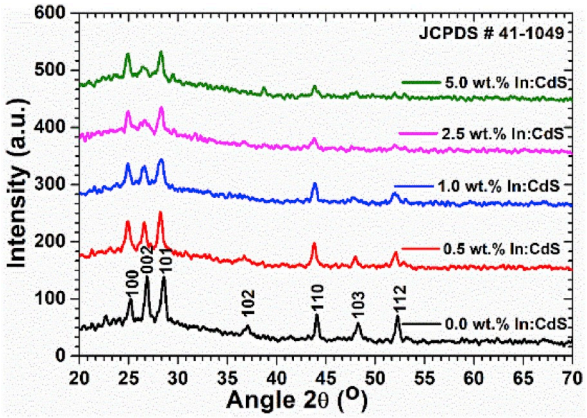

Fig. 1. XRD patterns of pure and In doped CdS films.

In recent past CdS in the form of thin films and nanopowders has been prepared with a number of dopants like: Na, K, Ni, Cu, Zr, Zn, Sm, Nd, Gd, La, Ga, Te, etc. [14–23]. These reports present a large-scale application of doped CdS. The CdS thin films have been fabricated using a number of techniques known as chemical bath deposition (CBD) [24,25], thermal evaporation [26], electron beam [27], RF sputtering [28], spin coating [29], electrodeposition/electrochemical [30,31], etc. In recent spray pyrolysis technique was employed by several authors and prepared the thin films of pure and doped CdS with modified structural and physical properties i.e. opto-electrical and nonlinear for a number of applications [12,15,32–38].

According to past literature the In doped CdS thin films were deposited by numerous authors, Atay et al. report the fabrication of 25, 35 and 45% In doped CdS films by ultrasonic spray pyrolysis method at 300 ± 5 °C and only investigate the structural-elemental-morphological and electrical properties [39]. Garcia-Cuenca et al. prepared the In doped CdS thin films by vacuum evaporation and mainly study the electrical properties [40]. Kim et al. fabricated the In doped CdS films using vacuum evaporation and subjected to investigate electrical parameters [41]. Perna et al. prepared films of In:CdS by pulse laser deposition and investigate structural-vibrational-optical and photoluminescence properties [42]. Hayashi et al. reports the fabrication of highly-conductive In: CdS films by co-evaporation method [43].

These reports also indicate the uniqueness of spray pyrolysis technique in obtaining the large area films with high homogeneity. Hence, the authors select the spray pyrolysis technique to obtain the good quality thin films. Though these report lacks the systematic low and high In doping effect on opto-electrical-nonlinear characteristics of CdS films. Hence, the authors studied the above-mentioned properties using a number of state-of-art experimental technique such as X-ray diffraction (XRD), energy dispersive X-ray spectroscopy/scanning electron microscopy mapping (EDX/SEM), ultraviolet–visible–near infrared spectroscopy (UV-VIS-NIR) and Z-scan measurements and discussed here.

2. Experimental details

2.1. Materials and thin films fabrication

For the preparation of solutions to fabricate In doped CdS films the following materials were procured from different companies, $CdCl_2$. H_2O, NH_3, thiourea, $In_2(SO_4)_3$. H_2O from Sigma Aldrich and HIMEDIA companies and used as it is. Initially $CdCl_2$ and thiourea was dissolved in double distilled water and NH_3 solvents by taking them in 4:1 separately. Then different concentrations of $In_2(SO_4)_3$. H_2O (0.0, 0.5, 1.0, 2.5, and 5.0 wt%) were liquified in double distilled water in dissimilar glass pots. Finally, all were mixed together under continuous stirring using a magnetic stirrer at room temperature. The pH was maintained to be 11.5 for all solutions. These all prepared solutions were used in spray pyrolysis technique and deposited the films on hot substrate at 300 °C. In spray pyrolysis system the detachment of nozzle and glass substrate was ~27 cm and pressure of gas carrier ~ 1 kg/m^2. The flow rate of solutions was kept constant at 5 ml/m. The thickness of finally prepared films was measured using a stylus profilometer and noted ~450 nm.

2.2. Characterization techniques

Shimadzu LabX XRD-6000, XRD system was used to record the XRD patterns in angular range of 20–70° at speed of 4°/m. To investigate the effect of In doping on vibrational modes of CdS we measured the FT-Raman spectra by THERMO SCIENTIFIC, DXR FT-RAMAN spectrophotometer by using the excitation wavelength of 532 nm at 8 mW laser power. For elemental composition and homogeneity confirmation of In dopant and surface morphology was studied using EDX/SEM mapping/SEM (JSM 6360 LA, Japan). A Lumina fluorescence spectrophotometer from Thermo Fisher Scientific was used to record photoluminescence spectra. UV-VIS-NIR absorbance, transmittance and reflectance spectra were recorded through a JASCO V-570, UV–VIS–NIR spectrophotometer. Z-scan measurement was carried out in both open and close aperture modes using 632.8 nm wavelength laser.

Table 1
Estimated values of lattice constants, L, δ and ε, N and TC for In doped CdS films.

Samples	a = b (Å)	c (Å)	V (Å)^3	L_{ave} (nm)	δ_{ave} (nm^{-2}) × 10^{-3}	$\varepsilon_{ave} \times 10^{-3}$	N × 10^4
0.0 wt% In:CdS	4.1427	6.7207	99.8881	19.669	2.863	1.822	3.987
0.5 wt% In:CdS	4.1391	6.7276	99.8176	19.353	2.913	1.847	3.800
1.0 wt% In:CdS	4.1403	6.7238	99.8154	18.784	2.976	1.877	3.475
2.5 wt% In:CdS	4.1443	6.7223	99.9907	18.622	3.041	1.894	3.380
5.0 wt% In:CdS	4.1373	6.7189	99.6037	16.062	6.056	2.527	2.177

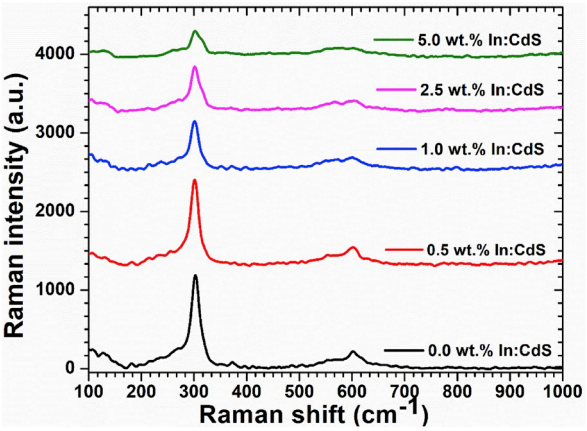

Fig. 2. Vibrational spectra for pure and In doped CdS films.

3. Results and discussion

3.1. XRD analysis

The recorded XRD patterns of pure and In doped CdS films are displayed in Fig. 1. Figure revealed that the grown films are polycrystalline in nature with considerable good crystallinity. It is also noticeable from figure that the intensity of XRD peaks is reducing with increasing the In content indicates low dimension crystallites formation in films. The major peaks in XRD pattern were indexed as (100), (200), (101), (102), (110), (103) and (112) with the help of standard XRD data JCPDS card No.: 41-1049. Hence, these indexing confirm the formation of hexagonal CdS system even at higher In doping content. Further, POWDERX software was employed to obtain lattice parameters of all films as given in Table 1, which further confirm the hexagonal phase. Also, by In doping content in CdS the lattice constants were noticed to be varied (see Table 1). The recorded XRD data was used to obtain angular position, full-width-half maximum, Intensity counts etc. which were used to determines average crystallite size (D_{ave}), density of dislocation (δ_{ave}), strain (ε_{ave}) and number of unit cells (N) in the films using well known relations [4,44–47]: $D_{ave} = \frac{0.9\lambda}{\beta_{2\theta}\ cos\theta}$, $\delta_{ave} = \frac{1}{D_{ave}^2}$, $\varepsilon_{ave} = \frac{\beta_{2\theta}\ cos\theta}{4}$, and $N = \frac{\pi D_{ave}^3}{6V}$, correspondingly. The average values of D_{ave}, δ_{ave}, and ε_{ave} estimated from all indexed planes are listed in Table 1. The data listed in Table 1 reveals that the D_{ave} value is decreasing from 20 to 16 nm with increasing the In doping content in CdS, hence δ_{ave} and ε_{ave} are varying accordingly. However, Atay et al. reports the crystallites size in range of 31–45 nm for 25, 35 and 45% In:CdS films and shows the reduction with In doping [39]. As the value of D_{ave} increases the δ_{ave} and ε_{ave} are decreasing in a systematic way indicate the reduction of defects in the films by In doping in CdS. The N values are also decreasing with increasing the In doping in CdS films. This is due to the change in D_{ave} and V values with In doping. All these parameters displayed that the films are getting more perfection with increasing In doping in CdS.

3.2. Vibrational spectroscopy study

Raman spectra for pure and In doped CdS films has been presented in Fig. 2. It is clearly visible in figure that by increasing the In content in CdS the Raman intensity of all peaks is decreasing which indicates low dimension grain formation in the films as revealed in XRD analysis. This may also confirm from increasing FWHM values of peaks. All vibrational spectra contain two major Raman modes at 302 ± 2 and 602 ± 3 cm^{-1} in all fabricated In:CdS films. The vibration modes are known as fundamental longitudinal optical (LO) phonon modes and ascribed as 1LO (302 ± 2 cm^{-1}) and first overtone, 2LO (602 ± 3 cm^{-1}) which are in agreement with earlier reports for CdS films and nanostructures [48–50]. The modes of vibrations are reported to be exist at 305 cm^{-1} (1LO) and 611 cm^{-1} (2LO) in bulk CdS [51,52], hence clearly revealed that there is a shift in peaks positions towards lower wavenumbers in currently fabricated films, which is due to nanosized grains formation in CdS [20].

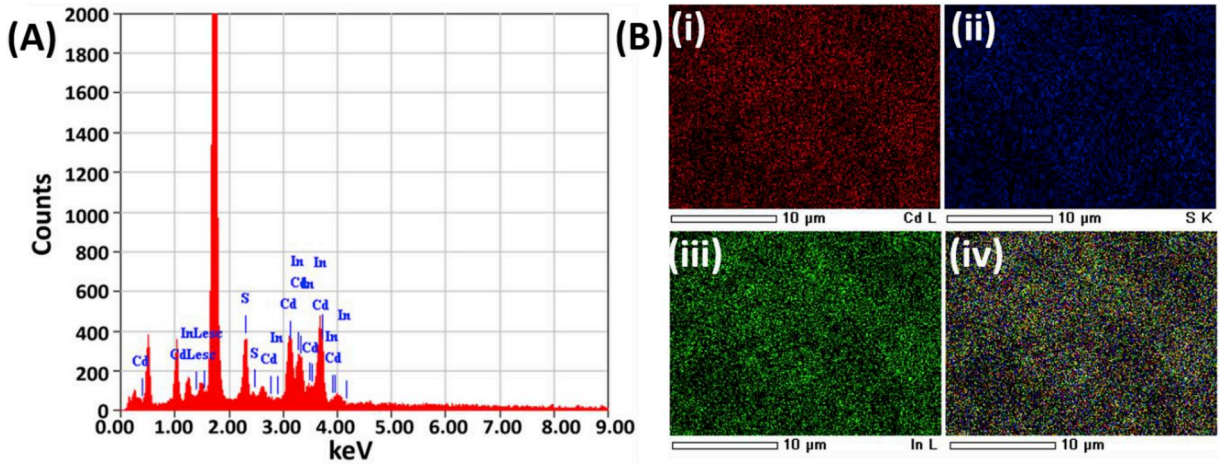

Fig. 3. EDX spectrum and SEM mapping image for 2.5 wt% In:CdS film.

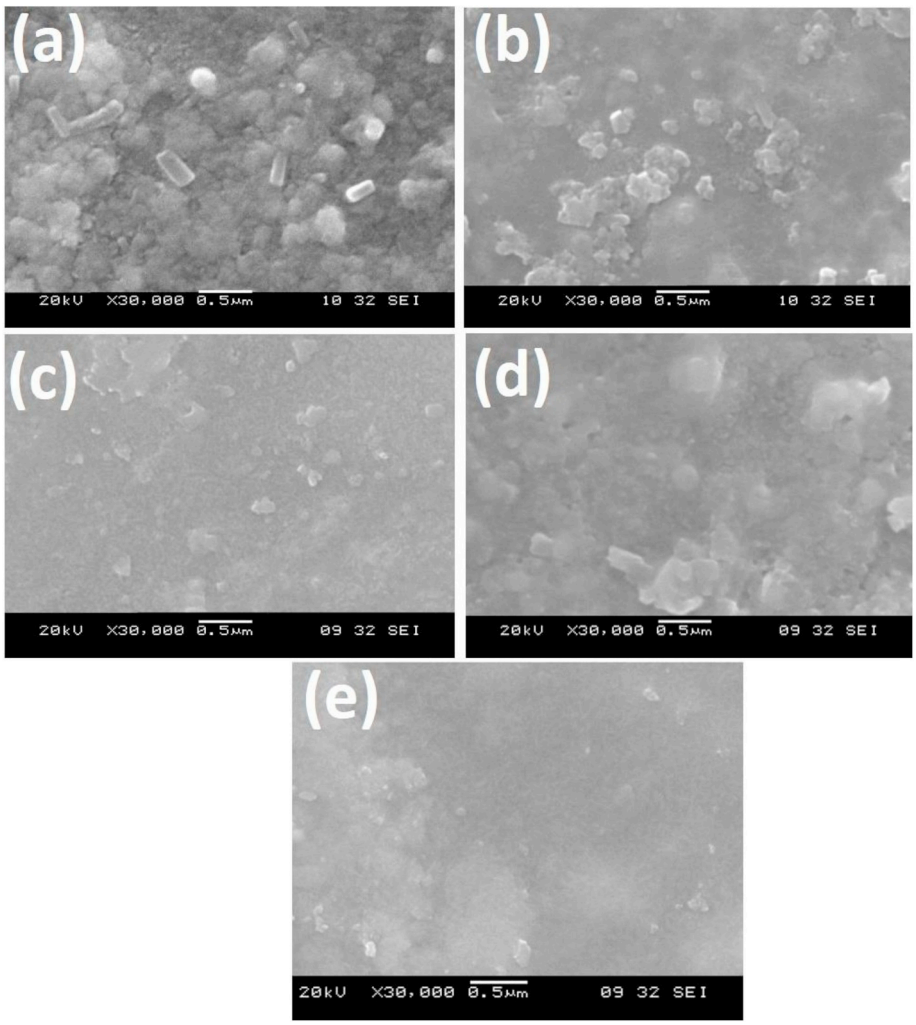

Fig. 4. SEM images for (a) pure, (b) 0.5 wt%, (c) 1.0 wt%, (d) 2.5 wt% and (e) 5.0 wt% In:CdS films.

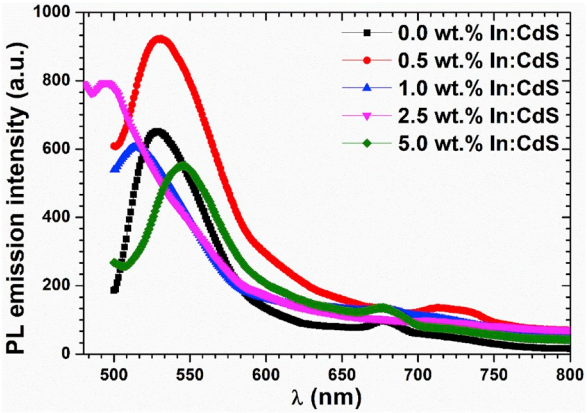

Fig. 5. Photoluminescence spectra for pure and In doped CdS films at $\lambda_{exc} = 450$ nm.

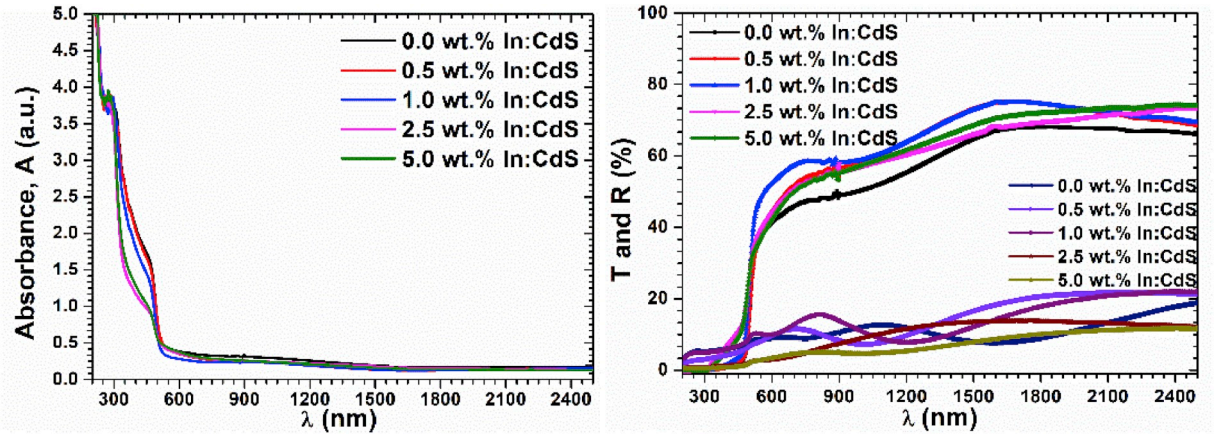

Fig. 6. Plots of (a) A, and (b) Transmittance and Reflectance spectra for all In:CdS films.

3.3. EDX/SEM mapping and morphological studies

To confirm the presence of In in 2.5 wt% In doped CdS film and its homogeneity the EDX and SEM mapping measurements were carried as shown in Fig. 3(A) and (B). The peak of In along with Cd and S can be seen in Fig. 3(A), indicates the In doping in films. Further SEM mapping revealed the homogeneous doping of In in CdS films as displayed in Fig. 3(B). Fig. 3(B) (i) is for Cd (red), (ii) is for S (blue) and (iii) is for In (green) and (iv) is for all together. Thus, Fig. 3(B)(iv) revealed that In has been doped unvaryingly in CdS as it is available all over the surface of the films. Hence, both EDX and SEM mapping confirm the In doping in CdS films.

The SEM micrographs for pure and In doped CdS films are exposed in Fig. 4(a–e). All SEM images revealed that the grown films are free from cracks or point holes, which are major issues in films and diminish the key properties. Also, the grains are formed in compact manner which are spread all over the films consistently indicating the thickness uniformity of films. Fig. 4(a) contains larger grains in pure CdS, however with In doping content the grains size is found to be reduced as clear from Fig. 4(b–e). The size of grain in pure CdS is in range of 20–30 nm, in 0.5 wt% In doped CdS, 18–22 nm, in 1.0 wt%, 2.5 wt% and 5.0 wt% In doped CdS in range of 10–15 nm. It may be mentioned here that the size of grains are averagely written here some minor variation may occur when the size will be measured with different software's. The grain size is in accordance to crystallite size determined in section 3.1. It is also noticeable here that the pure and 0.5 wt% In doped CdS films are having nanoclusters formation however when In doping content increased the cluster formation disappears and films becomes more compact with lower grain size. In previous report on In:CdS by Atay et al. the cluster formation is more when In doping was taken place [39].

3.4. Photoluminescence analysis

All the In:CdS films were subjected to excite at 450 nm wavelength to record the PL emission spectra as shown in Fig. 5. The emission intensity is found to be varied with In doping content in CdS. The emission intensity of 1.0 wt% In doped CdS is found to be highest indicated more defects in the film. However, it is reducing with increasing the In content but not systematically. The lowest intensity was observed for 5.0 wt% In doped CdS films indicates low defects. These results are in semi agreement with XRD and Raman

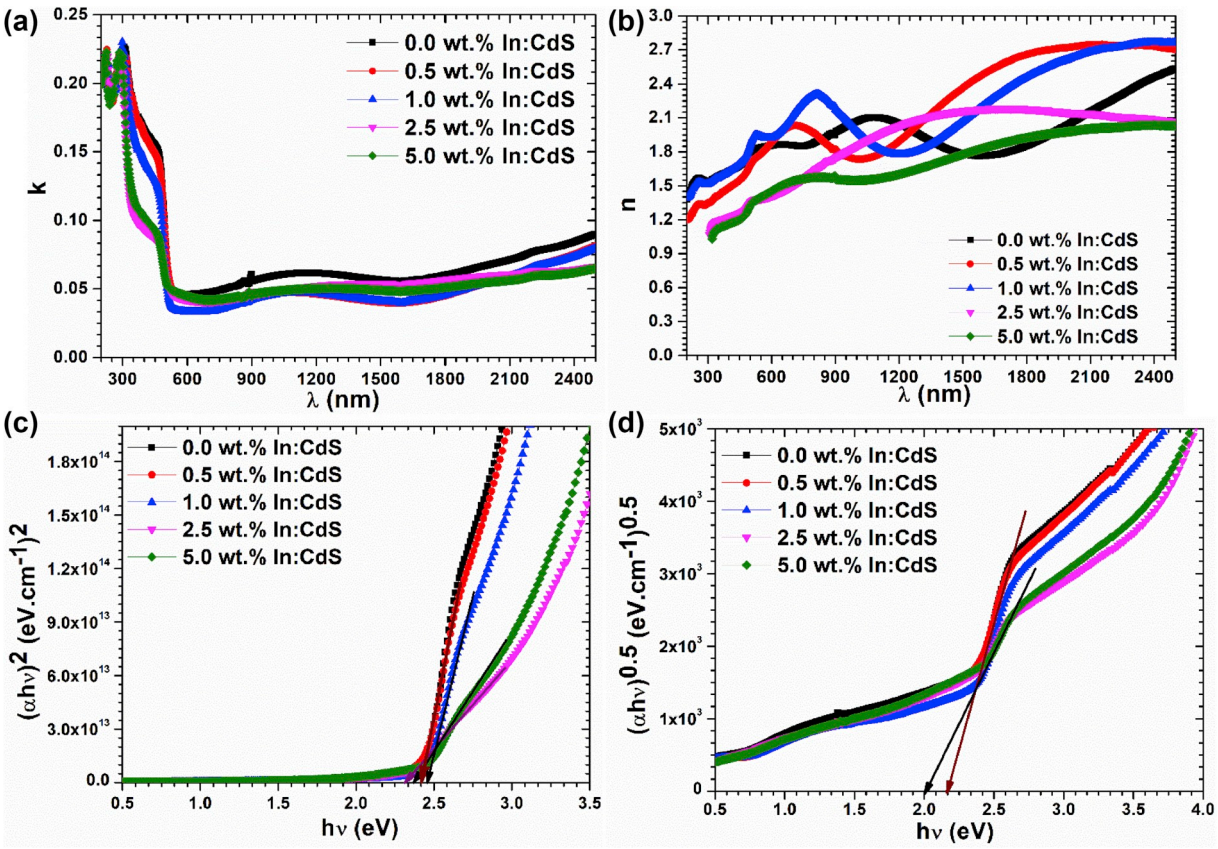

Fig. 7. Plots of (a) k, (b) n, (c) $(\alpha h\upsilon)^2$ vs. $h\upsilon$ and (d) $(\alpha h\upsilon)^{0.5}$ vs. $h\upsilon$ for all In:CdS films.

results. PL emission spectra possess a single intense green emission band at 529, 530, 516, 495, 545 nm for pure, 0.5, 1.0, 2.5, and 5.0 wt% In:CdS film. This shows that the emission peak position is changing with increasing the In content in CdS. This might be owing to deep level defects arises from disorderness in structure when In doping taking place in CdS. The energy band gap estimated from PL spectra is found in range of 2.50 to 2.28 eV for 5.0 wt% In:CdS films. The observed PL emission peak is in agreement with previous report on doped CdS in range of 510–600 nm [20,21]. This emission ascribed to band to band emission or emission owing to formation of defects by In doping in CdS.

3.5. UV–Vis–NIR spectroscopy study

3.5.1. A, T and R analyses

The measured A, T and R spectra for all In:CdS films are exposed in Fig. 6 (a) and (b). The figure (a) shows that the films are having very sharp absorption edge which is a normal trend in semiconducting materials. Fig. (b) indicates that the grown films are having low transparency in 550–1100 nm region which increased afterwards. Such kind of modification in transparency of grown films might evolve owing to change in surface morphology and size of crystallites in the films [53]. The measured reflectance shown in Fig. (b) is also showing similar behaviour to transmittance. Such non-systematic behaviour of transmission and reflection was also observed previously in In:CdS films [42].

3.5.2. k, n, E_g^d, and E_g^i analyses

Using the A, T and R data the absorption index, k, and refractive index, n, values were determined using the following rules [4,47,54,55]: $k = \frac{\alpha\lambda}{4\pi}$ and $n = \frac{(1+R)}{(1-R)} + \sqrt{\frac{4R}{(1-R)^2} - k^2}$. The estimated values of k and n are plotted as a function of wavelength as exposed in Fig. 7 (a) and (b). The value of k was noticed in range from 0.025 to 0.23 in 200–2500 nm wavelength region. The value of k is reduced compared to pure with In doping content in range of 550 nm–2500 nm. The n values for pure and In doped CdS films were found in range from 1 to 2.8 and shows a strong effect of In doping content on CdS films. The currently estimated values are in good correlation with previous reports on CdS [56,57]. Now we focused to determine the band gap of all films in direct and indirect modes from Tauc's equation [5,58,59]: $(\alpha h\upsilon)^{1/s} = A(h\upsilon - E_g)$, all used symbols are well-explained in these references. The values of α for all films were estimated by: $\alpha = 2.303\frac{\text{Absorbance}}{t}$, t stand for thickness of films. The value of s has been selected as 1/2 and 2 in respect of direct and

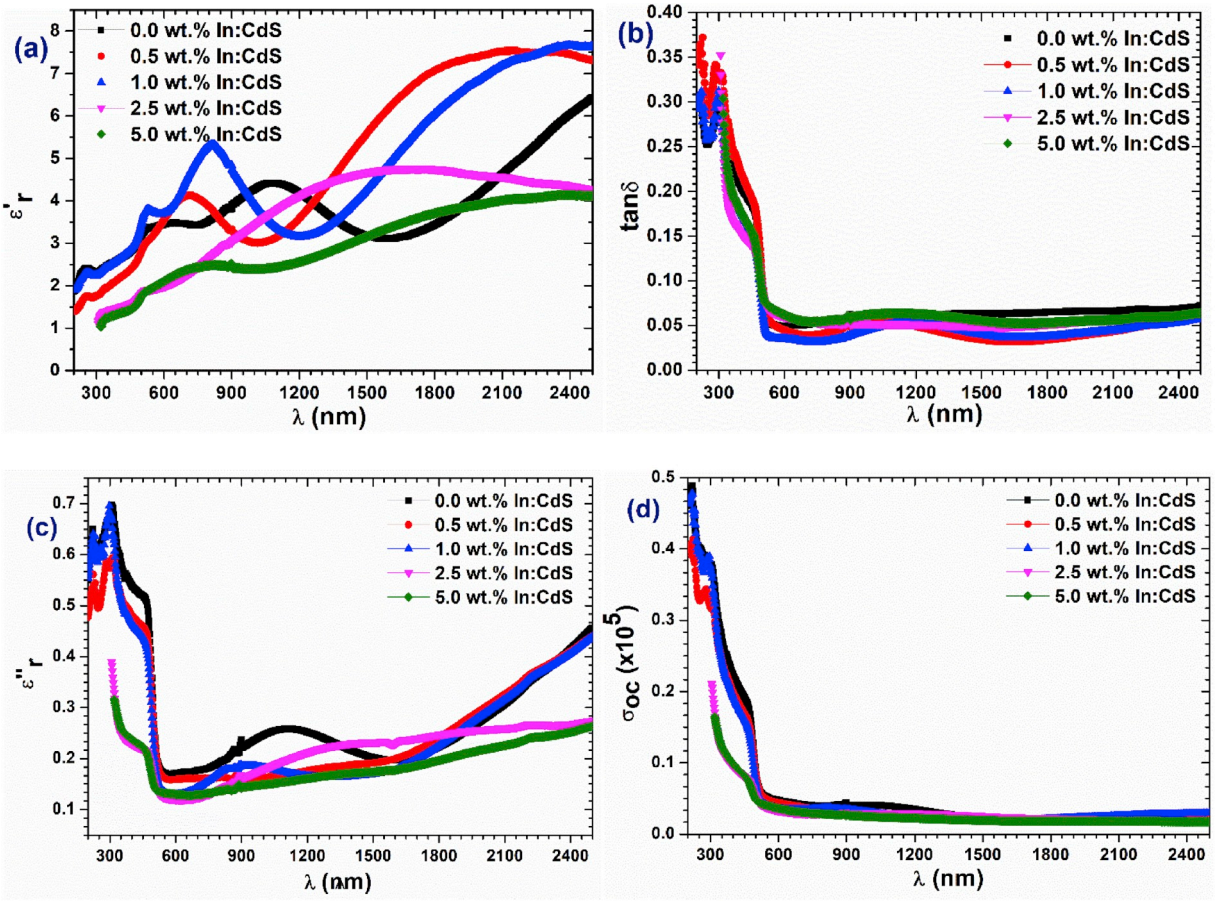

Fig. 8. Plots of (a) ε'_r vs. λ, (b) tanδ (c) ε''_r vs. λ, and (d) σ_{oc} vs. λ for all In:CdS films.

indirect energy gap. Finally, $(\alpha h\upsilon)^2$ and $(\alpha h\upsilon)^{1/2}$ values were determined and graphed with respect to $h\upsilon$ axis as revealed in Fig. 7(c) and (d), congruently. For obtaining the direct and indirect energy gap values a straight line towards the x-axis ($h\upsilon$) at $(\alpha h\upsilon)^2 = 0$ (see in figure c) and $(\alpha h\upsilon)^{1/2} = 0$ (see in figure d). The direct and indirect band gap values are noticed in 2.31–2.46 eV and 2.0–2.16 eV range, in that order. Both direct and indirect energy gap values are reducing with In doping and found in relation with previous reported values on CdS [60,61].

3.6. Dielectric, electrical and nonlinear optical studies

The dielectric constant values of its real (ε'_r) and imaginary parts (ε''_r) along with loss tangent (*tan*δ) were determined for pure and In doped CdS films. Because these constraints are highly applicable in defining the applications of films in capacitive storage, CMOS, DRAM devices [62–64]. Hence, the ε'_r and ε''_r in complex form are defined as: $\varepsilon = \varepsilon'_r + i\varepsilon''_r$ and here ε'_r and ε''_r are determined using [65]: $\varepsilon'_r = n^2 - k^2$ and $\varepsilon''_r = 2nk$. The estimated values of ε'_r, *tan*δ and ε''_r with respect to wavelength are exposed in Fig. 8(a) and (c) along with *tan*δ values in Fig. 8(b). The values of ε'_r, *tan*δ and ε''_r are noted in range of 1–8, 0.022 to 0.37, and 0.1 to 0.7, congruently in all tested wavelength range and observed to be comparable to earlier reported values [56]. The low values of tanδ and ε''_r signify the low number of defects in the fabricated films. The optical conductivity (σ_{oc}) values were also estimated using $\sigma_{oc} = \frac{\alpha nc}{4\pi}$ for all films and plotted in Fig. 8(d). It can be seen in figure that the value of σ_{oc} is reducing with increasing the wavelength in pure as well as doped CdS films and is of the order of 10^5 which indicates better conductive films.

3.7. Z-scan studies

The Z-scan technique developed by Bahae et al. [66] is the efficient tool to probe the optical properties of third order that dwells up in the sample when the incident beam of light is of sufficiently high intensity and frequency. Z-scan of 0.5, 1.0, 2.5 and 5.0 wt% In-CdS thin film has been done using the CW He-Ne laser operating at 632.8 nm. The thin film samples are placed at the focus position (Z = 0) and output intensity of the transmitted beam was successively recorded using the far field photo-detector. The close aperture Z-scan

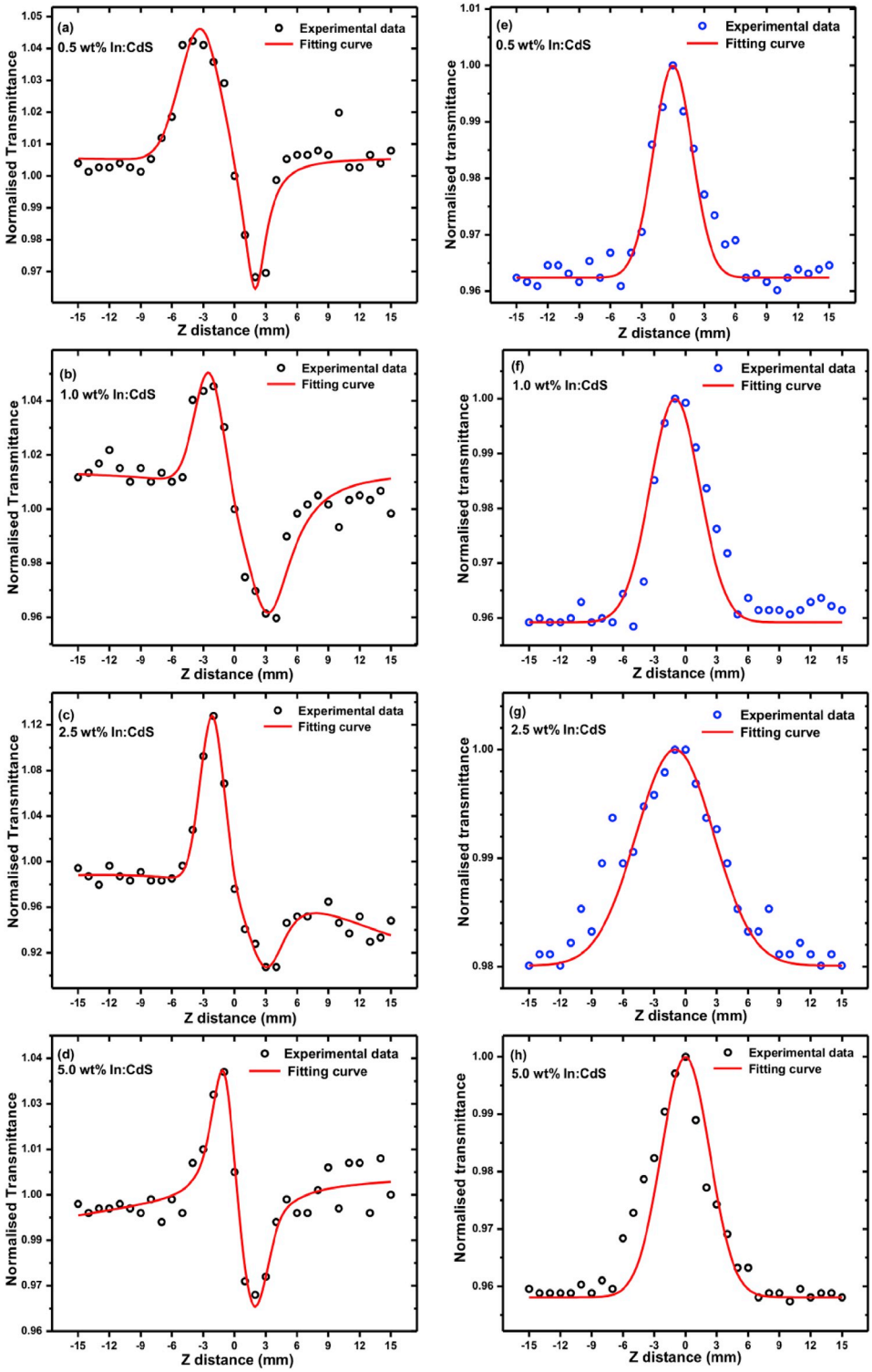

Fig. 9. Close (a, b, c, d) and open (e, f, g, h) aperture Z-scan profile of In:CdS thin film.

analysis has been performed to evaluate the nature of third order nonlinear optical (TONLO) refractive index (denoted by n_2) of thin film. It is noted that as the sample thin film is translated along the beam irradiated path the In-CdS thin films offer a pre-focus maximum to post-focus minima indicating the inheritance of negative nonlinear refraction [67]. The designing of optical night vision sensing devices highly demand the materials offering the negative n_2 profile [68–70]. The phase change in TONLO refractive

Table 2
TONLO parameters for In:CdS films.

Thin film	n_2 (cm^2/W)	β (cm/W)	χ^3 (esu)
0.5 wt% In:CdS	2.14×10^{-7}	3.12×10^{-3}	4.67×10^{-1}
1.0 wt% In:CdS	2.59×10^{-7}	3.99×10^{-3}	5.81×10^{-1}
2.5 wt% In:CdS	3.32×10^{-7}	4.75×10^{-3}	6.17×10^{-1}
5.0 wt% In:CdS	4.99×10^{-7}	5.37×10^{-3}	7.01×10^{-1}

index of given sample is governed by the repetitive irradiation of localized field of sample by high frequency laser beam which in turns leads to energy gradient along the sample surface making it to perform analogous to thermal lensing effect [71–73]. The open aperture Z-scan transmittance curve reveals that the In:CdS films express saturable absorption effect [74]. The occurrence of saturable absorption is stimulated owing to dominance of linear absorption coefficient over the excited state absorption coefficient [73,75]. It is notable that the CdS thin film offers the positive TONLO refractive index and reverse saturable absorption effect [10] while doping of In in CdS has altered the profile of n_2 as well as nonlinear absorption (β) as evident from Fig. 9. The magnitude of susceptibility highlights the polarizing strength [76] of the material and it is found that the TONLO susceptibility of In:CdS films increases successively with increase in concentration of In. The magnitudes of TONLO parameters have been evaluated using the standard formulae reported in literature [66] which are discussed in Table 2.

4. Conclusion

Good quality thin films of pure and 0.5, 1.0, 2.5, and 5.0 wt% In doped CdS films has been successfully fabricated using cost effective spray pyrolysis technique. Hexagonal crystal system of the grown films was approved by XRD and FT-Raman spectroscopy analyses. The crystallinity of films is noticed to be reduced with increasing the In content in CdS which indicates the reduction in size of particles. Hence, the values of crystallite size were estimated and noted to be reduced from 20 to 18 nm. Vibrational modes are found to be shifted by In doping in CdS owing to reduced particle size. The presence of In and its homogeneity in CdS film was confirmed from EDX/SEM elemental mapping study. The size of grains and nanoclusters formation are found to be reduced with increasing the amount of In content in CdS. The PL emission spectra comprises an intense green emission band at 529, 530, 516, 495, 545 nm in pure, 0.5, 1.0, 2.5, and 5.0 wt% In:CdS film, in that order. The grown films are found to be of good optical transparency vis. In range of 65%–75%. The value of direct energy gap was noticed in range of 2.31–2.46 eV and reduction was observed with In doping content. The Z-scan study in both open and closed aperture conditions was done and β, χ^3 and n_2 values were determined in range from 3.12×10^{-3} to 5.37×10^{-3} cm/W, 4.67×10^{-1} to 7.01×10^{-1} esu and 2.14×10^{-7} to 5.99×10^{-7} cm^2/W, correspondingly. The enhanced values of nonlinear characteristics makes the films highly applicable for device applications.

Conflicts of interest

Authors have no conflict of interest to show.

Acknowledgement

The authors would like to express their gratitude to Deanship of Scientific Research at King Khalid University for funding this work through Research Groups Program under Grant No. R.G.P. 2/42/40.

References

[1] C. Lee, K. Lim, J. Song, Highly textured ZnO thin films doped with indium prepared by the pyrosol method, Sol. Energy Mater. Sol. Cells 43 (1996) 37–45.
[2] P.M.R. Kumar, C.S. Kartha, K.P. Vijayakumar, T. Abe, Y. Kashiwaba, F. Singh, D.K. Avasthi, On the properties of indium doped ZnO thin films, Semicond. Sci. Technol. 20 (2005) 120.
[3] M. Benhaliliba, C. Benouis, M. Aida, F. Yakuphanoglu, A.S. Juarez, Indium and aluminium-doped ZnO thin films deposited onto FTO substrates: nanostructure, optical, photoluminescence and electrical properties, J. Sol. Gel Sci. Technol. 55 (2010) 335–342.
[4] M. Shkir, A. Khan, A.M. El-Toni, A. Aldalbahi, I.S. Yahia, S. AlFaify, Structural, morphological, opto-nonlinear-limiting studies on Dy:PbI2/FTO thin films derived facilely by spin coating technique for optoelectronic technology, J. Phys. Chem. Solids 130 (2019) 189–196.
[5] M. Shkir, M.T. Khan, S. AlFaify, Novel Nd-doping effect on structural, morphological, optical, and electrical properties of facilely fabricated PbI2 thin films applicable to optoelectronic devices, Appl. Nanosci. (2019), https://doi.org/10.1007/s13204-019-00983-w.
[6] F. Khodam, A.R. Amani-Ghadim, S. Aber, Preparation of CdS quantum dot sensitized solar cell based on ZnTi-layered double hydroxide photoanode to enhance photovoltaic properties, Sol. Energy 181 (2019) 325–332.
[7] F. Göde, S. Ünlü, Synthesis and characterization of CdS window layers for PbS thin film solar cells, Mater. Sci. Semicond. Process. 90 (2019) 92–100.
[8] K. Ramanathan, M.A. Contreras, C.L. Perkins, S. Asher, F.S. Hasoon, J. Keane, D. Young, M. Romero, W. Metzger, R. Noufi, Properties of 19.2% efficiency ZnO/CdS/CuInGaSe2 thin-film solar cells, Prog. Photovolt. Res. Appl. 11 (2003) 225–230.
[9] Y. Zhao, M. Yuan, Y. Chen, Y. Huang, J. Lian, S. Cao, H. Li, L. Wu, Size controllable preparation of sphere-based monolayer CdS thin films for white-light photodetectors, Ceram. Int. 44 (2018) 2407–2412.
[10] R.A. Ismail, A.-M.E. Al-Samarai, A.Y. Ali, Preparation and characteristics study of CdS/macroporous silicon/c-Si double heterojunction photodetector by spray pyrolysis technique, Optik 168 (2018) 302–312.
[11] S. Mathew, B. Samuel, A. Mujeeb, M. Kailasnath, V.P.N. Nampoori, C.P. Girijavallabhan, Effect of Au coating on optical properties of CdS nanoparticles and their optical limiting studies, Opt. Mater. 72 (2017) 673–679.

[12] R. Bairy, A. Jayarama, G.K. Shivakumar, S.D. Kulkarni, S.R. Maidur, P.S. Patil, Effect of Aluminium doping on photoluminescence and third-order nonlinear optical properties of nanostructured CdS thin films for photonic device applications, Phys. B Condens. Matter 555 (2019) 145–151.
[13] Y. Ye, L. Dai, X. Wen, P. Wu, R. Pen, G. Qin, High-Performance single CdS nanobelt metal-semiconductor field-effect transistor-based photodetectors, ACS Appl. Mater. Interfaces 2 (2010) 2724–2727.
[14] S. Mageswari, L. Dhivya, B. Palanivel, R. Murugan, Structural, morphological and optical properties of Na and K dual doped CdS thin film, J. Alloy. Comp. 545 (2012) 41–45.
[15] A. Rmili, F. Ouachtari, A. Bouaoud, A. Louardi, T. Chtouki, B. Elidrissi, H. Erguig, Structural, optical and electrical properties of Ni-doped CdS thin films prepared by spray pyrolysis, J. Alloy. Comp. 557 (2013) 53–59.
[16] R. Panda, V. Rathore, M. Rathore, V. Shelke, N. Badera, L.S. Chandra, D. Jain, M. Gangrade, T. Shripati, V. Ganesan, Carrier recombination in Cu doped CdS thin films: photocurrent and optical studies, Appl. Surf. Sci. 258 (2012) 5086–5093.
[17] V. Narasimman, V. Nagarethinam, K. Usharani, A. Balu, Optoelectronic, magnetic and antibacterial properties of Zr-doped CdS thin films, Optik-Int. J. Light Electron Opt. 138 (2017) 398–406.
[18] L.A. González, I. Carreón-Moncada, M.A. Quevedo-López, Negative differential resistance as effect of Zn doping of chemically processed CdS thin film transistors, Mater. Lett. 192 (2017) 161–164.
[19] S. L, J. R, P. A, L. Jih-Hsin, M. Hsin-Yuan, Synthesis, structural and optical properties of Sm3+ and Nd3+ doped cadmium sulfide nanocrystals, Mater. Res. Bull. 52 (2014) 128–133.
[20] A. Khan, M. Shkir, M.A. Manthrammel, V. Ganesh, I.S. Yahia, M. Ahmed, A.M. El-Toni, A. Aldalbahi, H. Ghaithan, S. AlFaify, Effect of Gd doping on structural, optical properties, photoluminescence and electrical characteristics of CdS nanoparticles for optoelectronics, Ceram. Int. 45 (2019) 10133–10141.
[21] M.A. Manthrammel, V. Ganesh, S. Mohd, I.S. Yahia, S. Alfaify, Facile synthesis of La-doped CdS nanoparticles by microwave assisted co-precipitation technique for optoelectronic application, Mater. Res. Express 6 (2019), 025022.
[22] S. Alhammadi, H. Jung, S. Kwon, H. Park, J.-J. Shim, M.H. Cho, M. Lee, J.S. Kim, W.K. Kim, Effect of Gallium doping on CdS thin film properties and corresponding Cu (InGa) Se2/CdS: Ga solar cell performance, Thin Solid Films 660 (2018) 207–212.
[23] R. Banerjee, S. Ray, A.K. Barua, Properties of tellurium doped vacuum evaporated CdS thin films, Jpn. J. Appl. Phys. 21 (1982) L43–L45.
[24] J. Hiie, T. Dedova, V. Valdna, K. Muska, Comparative study of nano-structured CdS thin films prepared by CBD and spray pyrolysis: annealing effect, Thin Solid Films 511 (2006) 443–447.
[25] A.J. Khimani, S.H. Chaki, T.J. Malek, J.P. Tailor, S.M. Chauhan, M. Deshpande, Cadmium sulphide (CdS) thin films deposited by chemical bath deposition (CBD) and dip coating techniques—a comparative study, Mater. Res. Express 5 (2018), 036406.
[26] P.P. Sahay, R.K. Nath, S. Tewari, Optical properties of thermally evaporated CdS thin films, Cryst. Res. Technol. 42 (2007) 275–280.
[27] S. Chander, M.S. Dhaka, Optical and structural constants of CdS thin films grown by electron beam vacuum evaporation for solar cells, Thin Solid Films 638 (2017) 179–188.
[28] C.T. Tsai, D.S. Chuu, G.L. Chen, S.L. Yang, Studies of grain size effects in rf sputtered CdS thin films, J. Appl. Phys. 79 (1996) 9105–9109.
[29] M.S. Deora, S. Sharma, Effect of incorporation of sulphur on the structural, morphological and optical studies of CdSe thin films deposited by solution processed spin coating technique, Thin Solid Films 670 (2019) 68–75.
[30] G. Sasikala, R. Dhanasekaran, C. Subramanian, Electrodeposition and optical characterisation of CdS thin films on ITO-coated glass, Thin Solid Films 302 (1997) 71–76.
[31] O.K. Echendu, S.Z. Werta, F.B. Dejene, K.O. Egbo, Structural, vibrational, optical, morphological and compositional properties of CdS films prepared by a low-cost electrochemical technique, J. Alloy. Comp. 778 (2019) 197–203.
[32] K. Karthik, S. Pushpa, M. Madhukara Naik, M. Vinuth, Influence of Sn and Mn on structural, optical and magnetic properties of spray pyrolysed CdS thin films, Mater. Res. Innov. (2019) 1–5.
[33] A.A. Aboud, A. Mukherjee, N. Revaprasadu, A.N. Mohamed, The effect of Cu-doping on CdS thin films deposited by the spray pyrolysis technique, J. Mater. Res. Technol. (2019).
[34] K.M. Saleh, Study influence of substrate temperature on optical properties of CdS thin films prepared by chemical spray pyrolysis, Ibn AL-Haitham J. Pure Appl. Sci. 32 (2019) 7–16.
[35] R. Murugesan, S. Sivakumar, K. Karthik, P. Anandan, M. Haris, Structural, optical and magnetic behaviors of Fe/Mn-doped and co-doped CdS thin films prepared by spray pyrolysis method, Appl. Phys. A 125 (2019) 281.
[36] C. Santiago Tepantlán, A. Pérez González, I. Valeriano Arreola, Structural, optical and electrical properties of CdS thin films obtained by spray pyrolysis, Rev. Mex. Fis. 54 (2008) 112–117.
[37] S. Yılmaz, The investigation of spray pyrolysis grown CdS thin films doped with fluorine atoms, Appl. Surf. Sci. 357 (2015) 873–879.
[38] S. Yılmaz, İ. Polat, M. Tomakin, E. Bacaksız, A research on growth and characterization of CdS:Eu thin films, Appl. Phys. A 125 (2019) 67.
[39] F. Atay, V. Bilgin, I. Akyuz, S. Kose, The effect of in doping on some physical properties of CdS films, Mater. Sci. Semicond. Process. 6 (2003) 197–203.
[40] M.V. Garcia-Cuenca, J.L. Morenza, J. Esteve, Electron tunneling in heavily In-doped polycrystalline CdS films, J. Appl. Phys. 56 (1984) 1738–1743.
[41] S.Y. Kim, D.S. Kim, B.T. Ahn, H.B. Im, Structural, electrical and optical properties of In-doped CdS thin films prepared by vacuum coevaporation, Thin Solid Films 229 (1993) 227–231.
[42] G. Perna, V. Capozzi, M. Ambrico, V. Augelli, T. Ligonzo, A. Minafra, L. Schiavulli, M. Pallara, Structural and optical characterization of undoped and indium-doped CdS films grown by pulsed laser deposition, Thin Solid Films 453–454 (2004) 187–194.
[43] T. Hayashi, T. Nishikura, T. Suzuki, Y. Ema, Formation and properties of In-doped high-conductivity CdS film, J. Appl. Phys. 64 (1988) 3542–3550.
[44] S. Mohd, Z.R. Khan, M.S. Hamdy, H. Algarni, S. AlFaify, A facile microwave-assisted synthesis of PbMoO 4 nanoparticles and their key characteristics analysis: a good contender for photocatalytic applications, Mater. Res. Express 5 (2018), 095032.
[45] M. Shkir, I.S. Yahia, M. Kilany, M.M. Abutalib, S. AlFaify, R. Darwish, Facile nanorods synthesis of KI:HAp and their structure-morphology, vibrational and bioactivity analyses for biomedical applications, Ceram. Int. 45 (2019) 50–55.
[46] M. Shkir, M. Kilany, I.S. Yahia, Facile microwave-assisted synthesis of tungsten-doped hydroxyapatite nanorods: a systematic structural, morphological, dielectric, radiation and microbial activity studies, Ceram. Int. 43 (2017) 14923–14931.
[47] M.T. Khan, M. Shkir, A. Almohammedi, S. AlFaify, Fabrication and characterization of La doped PbI2 nanostructured thin films for opto-electronic applications, Solid State Sci. 90 (2019) 95–101.
[48] H.L. Lee, I.A. Mohammed, M. Belmahi, M.B. Assouar, H. Rinnert, M. Alnot, Thermal and optical properties of CdS nanoparticles in thermotropic liquid crystal monomers, Materials 3 (2010) 2069–2086.
[49] C. Hu, X. Zeng, J. Cui, H. Chen, J. Lu, Size effects of Raman and photoluminescence spectra of CdS nanobelts, J. Phys. Chem. C 117 (2013) 20998–21005.
[50] H.I. Salim, O.I. Olusola, A.A. Ojo, K.A. Urasov, M.B. Dergacheva, I.M. Dharmadasa, Electrodeposition and characterisation of CdS thin films using thiourea precursor for application in solar cells, J. Mater. Sci. Mater. Electron. 27 (2016) 6786–6799.
[51] D.-S. Chuu, C.-M. Dai, Quantum size effects in CdS thin films, Phys. Rev. B 45 (1992) 11805.
[52] R. Rossetti, S. Nakahara, L.E. Brus, Quantum size effects in the redox potentials, resonance Raman spectra, and electronic spectra of CdS crystallites in aqueous solution, J. Chem. Phys. 79 (1983) 1086–1088.
[53] A. Mondal, T.K. Chaudhuri, P. Pramanik, Deposition of cadmium chalcogenide thin films by a solution growth technique using triethanolamine as a complexing agent, Sol. Energy Mater. 7 (1983) 431–438.
[54] M. Arif, M. Shkir, S. AlFaify, A. Sanger, P.M. Vilarinho, A. Singh, Linear and nonlinear optical investigations of N:ZnO/ITO thin films system for opto-electronic functions, Opt. Laser. Technol. 112 (2019) 539–547.
[55] M. Shkir, S. AlFaify, Effect of Gd3+ doping on structural, morphological, optical, dielectric, and nonlinear optical properties of high-quality PbI2 thin films for optoelectronic applications, J. Mater. Res., 1-10.

[56] Z.R. Khan, M. Shkir, V. Ganesh, S. AlFaify, I.S. Yahia, H.Y. Zahran, Linear and nonlinear optics of CBD grown nanocrystalline F doped CdS thin films for optoelectronic applications: an effect of thickness, J. Electron. Mater. 47 (2018) 5386–5395.
[57] Z.R. Khan, M. Shkir, A.S. Alshammari, V. Ganesh, S. AlFaify, M. Gandouzi, Structural, linear and third order nonlinear optical properties of sol-gel grown Ag-CdS nanocrystalline thin films, J. Electron. Mater. (2019) 1–11.
[58] S. AlFaify, M. Shkir, A facile one pot synthesis of novel pure and Cd doped PbI2 nanostructures for electro-optic and radiation detection applications, Opt. Mater. 88 (2019) 417–423.
[59] S. Alfaify, M. Shkir, A one pot room temperature synthesis of pure and Zn doped PbI2 nanostructures and their structural, morphological, optical, dielectric and radiation studies, J. Nanoelectron. Optoelectron. 14 (2019) 255–260.
[60] A. Cortes, H. Gómez, R.E. Marotti, G. Riveros, E.A. Dalchiele, Grain size dependence of the bandgap in chemical bath deposited CdS thin films, Sol. Energy Mater. Sol. Cells 82 (2004) 21–34.
[61] O. Zelaya-Angel, L. Hernandez, O. de Melo, J.J. Alvarado-Gil, R. Lozada-Morales, C. Falcony, H. Vargas, R. Ramirez-Bon, Band-gap shift in CdS: phase transition from cubic to hexagonal on thermal annealing, Vacuum 46 (1995) 1083–1085.
[62] K. Usha, R. Sivakumar, C. Sanjeeviraja, Optical constants and dispersion energy parameters of NiO thin films prepared by radio frequency magnetron sputtering technique, J. Appl. Phys. 114 (2013) 123501.
[63] D. Panda, T.-Y. Tseng, Growth, dielectric properties, and memory device applications of ZrO2 thin films, Thin Solid Films 531 (2013) 1–20.
[64] M.V. Fischetti, W.G. Vandenberghe, Dielectric properties of semiconductors, in: Advanced Physics of Electron Transport in Semiconductors and Nanostructures, Springer, 2016, pp. 223–251.
[65] M.-S. Kim, K.-G. Yim, J.-S. Son, J.-Y. Leem, Effects of Al concentration on structural and optical properties of Al-doped ZnO thin films, Bull. Korean Chem. Soc. 33 (2012) 1235–1241.
[66] M. Sheik-Bahae, A.A. Said, T.-H. Wei, D.J. Hagan, E.W. Van Stryland, Sensitive measurement of optical nonlinearities using a single beam, Quantum Electronics, IEEE J. 26 (1990) 760–769.
[67] G. Ravinder, C. Sreelatha, V. Ganesh, M. Shkir, M.A. Anis, C.R. Rao, Thickness-dependent structural, spectral, linear, nonlinear and z-scan optical studies of V 2 O 5 thin films prepared by a low-cost sol-gel spin coating technique, Mater. Res. Express (2019).
[68] M. Shkir, P.S. Patil, M. Arora, S. AlFaify, H. Algarni, An experimental and theoretical study on a novel donor-π-acceptor bridge type 2, 4, 5-trimethoxy-4′-chlorochalcone for optoelectronic applications: a dual approach, Spectrochim. Acta A Mol. Biomol. Spectrosc. (2016).
[69] S.R. Maidur, P.S. Patil, S.V. Rao, M. Shkir, S. Dharmaprakash, Experimental and computational studies on second-and third-order nonlinear optical properties of a novel D-π-A type chalcone derivative: 3-(4-methoxyphenyl)-1-(4-nitrophenyl) prop-2-en-1-one, Opt. Laser. Technol. 97 (2017) 219–228.
[70] Z.S. Fadhul, E.A. Ali, S.R. Maidur, P.S. Patil, M. Shkir, F.Z. Henari, Thermally induced optical nonlinearity and optical power limiting action of 2, 4, 5-trimethoxy-4′-nitrochalcone under CW laser regime, J. Nonlinear Opt. Phys. Mater. 27 (2018) 1850012.
[71] S. Azhar, M. Anis, G. Rabbani, M. Shirsat, M. Baig, S. Hussaini, S. AlFaify, M.A. Khan, Growth of NH4H2PO4 crystal in urea environment to optimize linear-nonlinear optical traits for photonic device applications, Optik 185 (2019) 1247–1252.
[72] B. Gu, H.-T. Wang, W. Ji, Z-scan technique for investigation of the noninstantaneous optical Kerr nonlinearity, Opt. Lett. 34 (2009) 2769–2771.
[73] M. Anis, G. Muley, M. Shkir, S. Alfaify, H. Ghramh, Comparative analysis on microhardness and third order nonlinear optical traits of pure and Nd3+ doped zinc tris-thiourea sulphate (ZTS) crystal, Mater. Sci.-Poland (2018).
[74] X. Wang, Q. Ren, H. Fan, J. Chen, Z. Sun, T. Li, X. Liu, G. Zhang, D. Xu, W. Liu, Preparation, crystal structure, spectrographic characterization, thermal and third order nonlinear optical properties of benzyltriethylamine bis (2-thioxo-1, 3-dithiole-4, 5-dithiolato) nickel (III), J. Cryst. Growth 312 (2010) 2206–2214.
[75] M. Anis, M. Shkir, M.I. Baig, S.P. Ramteke, G.G. Muley, S. AlFaify, H.A. Ghramh, Experimental and computational studies of L-tartaric acid single crystal grown at optimized pH, J. Mol. Struct. 1170 (2018) 151–159.
[76] P.S. Patil, S.R. Maidur, M. Shkir, S. AlFaify, V. Ganesh, K.N. Krishnakanth, S.V. Rao, Crystal growth and characterization of second-and third-order nonlinear optical chalcone derivative:(2E)-3-(5-bromo-2-thienyl)-1-(4-nitrophenyl) prop-2-en-1-one, J. Appl. Crystallogr. (2018) 51.